

Identifying resilient-important elements in interdependent critical infrastructures by sensitivity analysis

Xing Liu

Chair on Systems Science and the Energy Challenge, Foundation Electricité de France (EDF)
Laboratoire Génie Industriel, CentraleSupélec, Université Paris-Saclay
3 Rue Joliot Curie, 91190 Gif-sur-Yvette, France

E-mail: xing.liu@centralesupelec.fr

Elisa Ferrario

School of Engineering, Pontificia Universidad Católica de Chile and National Research Center for Integrated Natural Disaster Management (CIGIDEN) CONICYT/FONDAP/15110017
Avenida Vicuña Mackenna 4860, Santiago, Chile.

Chair on Systems Science and the Energy Challenge, Foundation Electricité de France (EDF)
Laboratoire Génie Industriel, CentraleSupélec, Université Paris-Saclay
3 Rue Joliot Curie, 91190 Gif-sur-Yvette, France

Email: elisa.ferrario@cigiden.cl

Enrico Zio

Chair on Systems Science and the Energetic Challenge, Foundation Electricité de France (EDF)
Laboratoire Génie Industriel, CentraleSupélec, Université Paris-Saclay
3 Rue Joliot Curie, 91190 Gif-sur-Yvette, France

Dipartimento di Energia - Politecnico di Milano
Via Ponzio 34/3, 20133 Milano, Italy

E-mail: enrico.zio@centralesupelec.fr, enrico.zio@polimi.it

Abstract: In interdependent critical infrastructures (ICIs), a disruptive event can affect multiple system elements and system resilience is greatly dependent on uncertain factors, related to system protection and restoration strategies. In this paper, we perform

sensitivity analysis (SA) supported by importance measures to identify the most relevant system parameters. Since a large number of simulations is required for accurate SA under different failure scenarios, the computational burden associated with the analysis may be impractical. To tackle this computational issue, we resort to two different approaches. In the first one, we replace the long-running dynamic equations with a fast-running Artificial Neural Network (ANN) regression model, optimally trained to approximate the response of the original system dynamic equations. In the second approach, we apply an ensemble-based method that aggregates three alternative SA indicators, which allows reducing the number of simulations required by a SA based on only one indicator. The methods are implemented into a case study consisting of interconnected gas and electric power networks. The effectiveness of these two approaches is compared with those obtained by a given data estimation SA approach. The outcomes of the analysis can provide useful insights to the shareholders and decision-makers on how to improve system resilience.

Keywords: Critical Infrastructure, System Resilience, Importance Measure, Sensitivity Analysis, Artificial Neural Networks, Ensemble of Methods

1 Introduction

The safety of critical infrastructures (CIs), such as electrical power grids, transportation, telecommunication, natural gas and oil, water supply networks and government services systems, are significantly threatened by multiple hazards, e.g., natural disasters [1,2] and human-made attacks [3]. Disruptive events that occur in one CI can trigger cascading failures to the interdependent CIs (ICIs), causing significant consequences and losses [4]. Then, how to anticipate, prepare for, respond to, and recover from disruptive events in CIs and ICIs, become important issues [6].

Resilience refers to the “ability of a system to *sustain* and *restore* its basic functionality following a hazard source or an event (even unknown)” [6]. Various attempts have been made to define, quantify, analyze and improve system resilience of CIs [7].

In scientific literature, works on system resilience mainly focus on the recovery aspect [8,9,10]. However, in practice, it is relevant to distinguish the individual contributions to system resilience from both the mitigation and recovery viewpoints in order to plan and implement the most effective strategies for improving resilience of ICIs. Indeed, the importance of a system element with respect to system resilience may change before, during and after the occurrence of a disruptive event, and, as a consequence, the associated resilience strategy may change too. Then, it is necessary to capture this

variation of criticality of the system elements to more efficiently guide the resilience strategies in the different phases following a disruptive event.

In this work, we model ICIs within a control-based dynamic modeling framework, as in [11], and we quantify three resilience measures for ICIs, introduced in [12], to analyze resilience in different phases, i.e., during the failure phase, the recovery phase, and the entire failure-recovery period. Then, we perform a sensitivity analysis (SA) that is able to account for the contribution of different sources of uncertainty in the model inputs (such as system design parameters and failure-recovery parameters) to the uncertainty in the outputs (such as resilience measures) [13]. SA can be performed to achieve different purposes such as [14,15]: 1) ranking, i.e., the identification of a ranking of the inputs on the basis of their contribution to the output variability, 2) screening, i.e., the identification of the inputs that have a non-influential effect to the output variability, and 3) mapping, i.e., the determination of the region of the space of input variability that produces relevant output values. In this work, the focus is on ranking; indeed, we perform SA to rank the inputs (parameters and elements of the ICIs) that are more critical with respect to the development and improvement of system resilience, in order to provide insights to the decision-makers. Identifying the most critical inputs to system resilience can support the implementation of appropriate resilience strategies and the effective improvement of system resilience.

Two types of SA approaches can be identified: local and global. Local (or differential) SA evaluates the effect on the output of small variations of the inputs around a reference value; the sensitivity indices typically used are partial derivatives or finite differences [15,16,17]. Global SA, instead, evaluates the effect on the output of inputs varying across the entire domain of possible input parameter variations; the sensitivity indices typically adopted are, e.g., correlation measures between inputs and outputs and statistical properties of the output distribution, such as variance [15]. Indicators for global SA are called global importance measures or uncertainty importance measures [18]. Local SA is straightforward, does not require many simulations, and its results are easily interpreted compared to global SA [17]; however, the latter one is considered more reliable [17] and offers higher capabilities [16]. Then, in this work, we focus on global SA.

Also, SA methods can be classified in different categories, for example [15] identified the following types of SA methods for environmental models: perturbation and derivative methods, multiple starts perturbation methods, correlation and regression analysis methods, Monte Carlo filtering, variance-based methods, density-based methods; [17] classified global SA methods for building energy analysis in four categories, i.e., regression methods, screening-based methods, variance-based methods, meta-model methods; [19] distinguished between screening methods, non-parametric (regression-based) methods, variance-based methods, density-based methods and expected-value-of-information-based

methods; [18] presented an overview of global SA techniques used in risk analysis, specifying three types of methods, i.e., non-parametric (regression-based) techniques, variance-based techniques and moment independent techniques. With respect to the last classification, in this paper, we consider both variance-based techniques and moment independent techniques for SA.

As mentioned above, global SA methods offer higher capabilities; however, they suffer of higher computational cost [16], since they explore the entire domain of inputs variability. As a result, the computational cost of the SA-driven importance measures (SADIM) can become very expensive, due to the long time needed by one single simulation to run and the large number of simulations required by SA. In order to reduce the computational burden of the analysis, we adopt two strategies: in the first one, we replace the long-running dynamic model with a fast-running regression model to reduce the time required by each simulation; in the second strategy, we keep the long-running dynamic model and adopt an ensemble-based method, which aggregates three SA indicators and allows obtaining accurate SA results with a lower number of simulations [16].

Fast-running regression models, also called metamodels (such as Artificial Neural Networks (ANNs) [20,21], Local Gaussian Processes (LGPs) [22-23], polynomial Response Surfaces (RSs) [24-25], polynomial chaos expansions [26-27], stochastic collocations [28], Support Vector Machines (SVMs) [29] and kriging [30,31,32]), can be built by means of input-output data examples to approximate the response of the original long-running dynamic models, and used to perform SA. Since the metamodel response is obtained quickly, the problem of high computational times is circumvented [33]. In this work, we use ANN-based metamodels to approximate the response of the long-running dynamic model and we apply SA by analyzing a variance-based sensitivity index (i.e., the first-order index) on the ANN model outputs.

The ensemble strategy allows integrating the output of three SA individual methods to generate reliable rankings, avoiding possible misinterpretations that can be produced by using a single SA method. This strategy has been shown to be particularly useful when the number of simulations needs to be reduced for computational issues [16]. The three SA indicators considered in this work are: 1) the first-order variance-based sensitivity measure (also called Pearson's correlation ratio or Sobol's first-order index) [19,34]; 2) the distribution-based sensitivity measure [18] and 3) the Beta measure on the basis of Kolmogorov-Smirnov distance [35]; while the first index is variance-based, the last two indices are given by moment independent techniques. To aggregate the results in the ensemble, we propose a normalized value sum aggregation method, derived from the ranking sum aggregation method [36]. In the rest of the paper, we refer to the first and second strategies as SADIM 1 and SADIM 2 approaches, respectively, for brevity. The results obtained from SADIM 1 and SADIM 2 are compared with those

obtained by a SA approach that estimates global sensitivity indices from given data, at the minimum computational cost, [19], to which we refer in the paper as “given data estimation method” or SADIM 3.

The present work is organized as follows. Section 2 presents the control-based modelling framework of ICIs and the system resilience indicators. Section 3 introduces the SADIM 1 and 2 approaches. In this Section, the basics of the ANN model, the definitions of the SA indicators and the aggregation strategy used in the ensemble-based approach are given. Section 4 illustrates the application of the proposed methodologies on a case study concerning interconnected gas and electric power networks. Finally, Section 5 draws conclusions from the work performed and presents the future works.

2 ICIs dynamic modelling framework and resilience metrics

In Section 2.1, we introduce a modelling framework for ICIs, where the system behaviors in the nominal operation and failure modes are described by a set of dynamic equations and the system states represent the level of a resource that passes through a given node or link of the ICIs. Accounting for the variability of users’ demands and the constraints on system states, we formulate an under-control flow distribution problem by a Model Predictive Control (MPC) algorithm to calculate the system states in real-time. In Section 2.2, we define the performance of the system. In Section 2.3, we present the uncertain system parameters that affect system resilience. In Section 2.4, we illustrate the system resilience metrics.

2.1 Modelling framework

In this work, ICIs are described as a network, on the basis of graph theory, and their operation is modeled by linear dynamic equations that describe the switching dynamic modes of the interconnected systems. Then, the modeling framework adopted is able to go beyond the purely topological description of a system by including dynamic aspects, although in a linearly (approximated) manner [11]. The ICIs model is quantified by simulation, reformulating it as an optimization problem, specifically into a look-ahead resource dispatch problem, which schedules the flows of resources within the ICIs based on up-to-date forecasts of users’ demands [12]. The MPC approach [37,38], which allows taking into account the constraints on system components, system control parameters, and system design parameters, has been adopted to identify the control actions at each time step [11,12].

In Section 2.1.1, the system dynamic equations are written in their state-space form (i.e., the linear time-invariant dynamic equations), where vectors of system state variables (x), controllable variables (u), disturbances (d), and system outputs (y) are related; in Section 2.1.2, the model constraints are illustrated; and in Section, 2.1.3, the model objective function is given.

2.1.1 Dynamics of ICIs

ICIs are represented as a networked graph, where the nodes are the subsystems, i.e., components or functional sets of components, and the links are physical, cyber or logical connections between the nodes [39]. Various resources are constantly produced, consumed, stored and transformed in the subsystems of the ICIs. Then, depending on the main functionalities of the nodes, i.e., production, consumption, storage, transportation and/or conversion, we classify them into suppliers, users, buffers, transporters, and convertors [11].

In the modelling framework, we consider as system states the levels of input flow, output flow and storage of the nodes, and the levels of input flow and output flow of the links connected to them. To mimic the realistic operations of ICIs under control, the outgoing links of buffering nodes and system driver nodes, as defined in [40], are considered as driver links and their output flows are designated as system controllable inputs. The general, discretized, state-space representation is written as follows [11]:

$$\begin{aligned} x(t+1) &= Ax(t) + Bu(t) + d(t) \\ y(t) &= Cx(t) \end{aligned}, \quad (1)$$

where $x = [x_1 \dots x_{N_x}]' \in R^{N_x}$ is the vector of the system states, $u = [u_1 \dots u_{N_u}]' \in R^{N_u}$ is the vector of the control variables, $y = [y_1 \dots y_{N_y}]' \in R^{N_y}$ is the vector of the system outputs, which are the flow levels received by the users, $d = [d_1 \dots d_{N_d}]' \in R^{N_d}$ is the vector of disturbance variables describing the losses of the system states due to the disruptions. The $N_x \times N_x$ matrix A contains the information on the system connectivity and, specifically, the rows and columns represent the nodes and the cells assume value 1 if the nodes on the rows depend on the nodes on the column, otherwise they assume value 0. The $N_u \times N_x$ ($N_u \leq N_x$) matrix B and the $N_y \times N_x$ matrix C represent the flow transmission coefficients, respectively. Matrix A is obtained from the topology of the system, whereas matrices B and C are given by the dynamic equations formulated for each component. Finally, the scale of time depends on the objective and level of detail of the analysis, on the type of system under analysis and also on the available input data. For example, in electric power networks, the scale of time when analyzing the unit commitment problem should be in minutes to analyze the ramping capabilities of power generators, whereas it can be in hours when analyzing the supply of electricity to customers. In this work, we consider an hourly resolution.

The advantage of using Eq. (1) is related to the possibility of describing the changes of flows during the failure and restoration processes, by explicitly representing the dynamic of flows on nodes and links.

This cannot be handled by the existing approaches of the classical, static network flow models [3,41].

The interested reader is referred to [11] and [12] for further details.

2.1.2 Constraints

The values of system states and control variables are limited by the capacities of the nodes and links. The constraints are formulated as follows:

$$0 < x(t) < CP_x, \quad (2)$$

$$0 < u(t) < CP_u, \quad (3)$$

where the elements in CP_x and CP_u take values of the capacities of the corresponding elements, i.e., the nodes or the links. In nominal operation, the capacity of an element i is at maximum level CP_i^N . When a disruptive event occurs, the capacity varies in time during the failure-recovery process, as shown in Figure 1:

$$CP_i(t) = CP_i^N - F_i + \mu_i(t - t_r), CP_i(t) \leq CP_i^N \quad (4)$$

with

$$F_i = \begin{cases} 0 & \text{for } 0 \leq t < t_f \\ \text{magnitude of failure} & \text{for } t \geq t_f \end{cases}, \quad (5)$$

$$\mu_i = \begin{cases} 0 & \text{for } 0 \leq t < t_r \\ \text{recovery rate} & \text{for } t \geq t_r \end{cases}. \quad (6)$$

where t_f is the time of failure and t_r is the start time of the recovery. The exact shape of the recovery function curve of an element is driven by the system resilience strategies. For example, [2] uses linear, trigonometric, and exponential recovery curves to represent the system response of average prepared, not well prepared and well prepared communities. For the sake of simplicity of illustration, here, we use linear recovery functions.

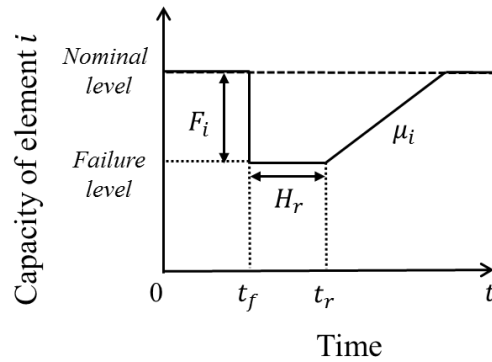


Figure 1 Evolution in time of the capacity of element i .

2.1.3 Objective function

Considering that the units of the resources in ICIs are different (e.g., for the gas network the unit is in

cubic feet **or m³** and for the electric power network it is in MW), we represent the level of relative insufficient satisfaction Y_{i_y} of user i_y , by a normalized and non-dimensional variable [11]:

$$Y_{i_y}(t) = \frac{D_{i_y}(t) - y_{i_y}(t)}{D_{i_y}(t)}, \quad (7)$$

where D_{i_y} is the demand of user i_y .

Based on the dynamic equations and constraints previously introduced, we use MPC algorithm to allocate the flows at each time step, **i.e., at each hour**. MPC performs a finite-horizon optimization by determining sequences of system states and control operations over a prediction horizon N_q for the minimization of the objective function at each time step within N_q , and, then, implementing only the first control action [42].

Here, the objective function is formulated to minimize the weighted sum of insufficiency function $Y_{i_y}(t)$ of user i_y , within the time horizon N_q :

$$\min \sum_{q=0}^{N_q} \left(\sum_{i_y \in N_y} \omega_{i_y} Y_{i_y}(t + q|t) \right), \quad (8)$$

where, ω_{i_y} is the weight assigned to the user i_y , and $\sum_{i_y} \omega_{i_y} = 1$.

By solving the optimization problem with MPC, the control action $u(t|t)$ is obtained from the control sequence:

$$u \triangleq \{u(t|t), u(t+1|t), \dots, u(t+N_q-1|t)\}. \quad (9)$$

Then, only the first control action $u(t|t)$ will be used in the recursion to calculate the system states at $t+1$.

2.2 System performance function

ICIs should provide stable and reliable services to the users; their performance can be defined from different perspectives (reliability, availability, resilience, safety, economics, etc.) and measured in **effective** ways, e.g., counting the number of operating components [2], the economic loss associated to the components and the casualties of people during the disaster [1]. According to [7], a measure of resilience of ICIs should be related to the capacity of enabling and enhancing people daily life. In this view, we evaluate the actual performance function of ICIs, $P(t)$, in terms of the weighted sum of the users states:

$$P(t) = \sum_{i_y}^{N_y} \omega_{i_y} y_{i_y}(t). \quad (10)$$

The performance reference function of the ICIs, $PR(t)$, is characterized as the weighted sum of the users demands:

$$PR(t) = \sum_{i_y}^{N_y} \omega_{i_y} D_{i_y}(t). \quad (11)$$

Under nominal operating conditions, the supply to each user, e.g., i_y , with respect to its demand D_{i_y} is always achieved, i.e., $y_{i_y}(t) = D_{i_y}(t)$ and $P(t)$ maintains values close to the performance reference function $PR(t)$.

2.3 Uncertain input variables

The uncertain inputs here considered to affect system resilience performance include system initial conditions, i.e., initial resource levels in the buffer subsystems, parameters of the process temporality, i.e., related to the process duration like the system response time and the time horizon, and parameters related to the failure-recovery process, i.e., failure magnitude and recovery rate.

The buffer subsystems in the ICIs contribute to system performance by storing resources, adjusting the supply of resources in nominal operation and compensating the insufficiency of resources in case of shortage during an accident. To include the functionality of the buffers, we assume that the initial inventory levels of buffers, $x_{BF_i}^{t=0}$, represents the initial resource level of buffer BF_i , at $t = 0$.

Two critical time durations are defined in a failure scenario: $H_r = t_r - t_f$ is the response time and $H_h = t_h - t_f$ is the time horizon, which represents the time within which the restoration is to be finished, where t_h is the time within which system performance is expected to return to the nominal level.

The failure magnitude F_i and recovery rate μ_i of an element i are considered as uncertain variables. The failure magnitude F_i is limited to the interval $[F_{i_{min}}, F_{i_{max}}] = [0, C_i]$, where C_i is its predefined capacity. The recovery rate μ_i varies within $[\mu_{i_{min}}, \mu_{i_{max}}]$, which can be, for example, $\mu_{i_{min}} = \frac{F_{i_{min}}}{H_{h_{max}}}$ and $\mu_{i_{max}} = \frac{F_{i_{max}}}{H_{h_{min}}}$.

2.4 System resilience metrics

Resilience can be described as a function of the system performance over time and it is typically represented by triangular [2,43,44] or trapezoidal [1] curves, as shown in Figure 2. As a result, the most used metrics for resilience quantification are usually based on area quantification, such as the area between the reference, $PR(t)$, and the actual, $P(t)$, system performance functions within a period of

interest, e.g., from the time of occurrence of a disruptive event until the complete recovery of the system [43,45].

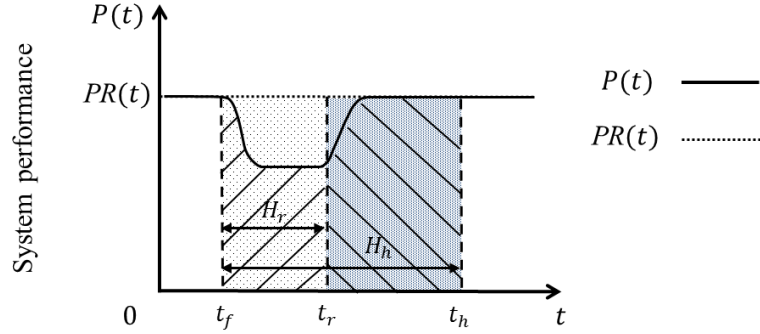


Figure 2 System performance following the occurrence of a disruptive event.

In this work, we compute resilience as a ratio of the areas between the actual, $P(t)$, and the reference, $PR(t)$, system performance functions during a given time period. Specifically, we consider three time periods that lead to the computation of three resilience metrics: 1) resilience by mitigation, R_m , during the disruptive (failure) phase of the system, from the time of occurrence of a disruptive event, t_f , until the time when the recovery starts, t_r ; 2) resilience by recovery, R_r , during the recovery phase of the system, from the time of starting of the recovery, t_r , to the time within which system performance is expected to return to the nominal level, t_h ; and 3) total resilience, R_t , during both the failure and recovery phases, i.e., from t_f until t_h .

The distinction between resilience by mitigation and resilience by recovery comes from the need of identifying the most important resilience protection and recovery activities that can contribute to the system resilience during the different phases of mitigation and recovery, following a disruptive event. Indeed, during the mitigation phase, the capacity of the system to maintain the nominal level of operation or mitigate the negative impacts of disruption mainly depends on the robustness and redundancy of the system, whereas in the recovery phase, the capacity of the system to return to its nominal operation following disruptive events mainly depends on the rapidity of the recovery and on the resourcefulness of the system [46]. However, it is worth mentioning that protection strategies implemented during the mitigation phase can contribute also to the system resilience during the recovery phase, indeed larger robustness and higher rapidity are correlated. In this work, this correlation is not considered when analyzing separately the mitigation and recovery phases, but it is included when analyzing the total resilience measure.

In the following, the mathematical formulation of the three resilience measures adopted is given.

The resilience by mitigation is quantified as the ratio of the area between the actual system performance function $P(t)$ and the time axis (the area shaded with upward diagonal stripes in Figure 2) for the time period $t_f \leq t \leq t_r$, and the area between the performance reference function $PR(t)$ and the time axis, for the time period $t_f \leq t \leq t_r$, which corresponds to the response time $H_r = t_r - t_f$, i.e., within the mitigation phase:

$$R_m = \frac{\int_{t_f}^{t_r} P(t) dt}{\int_{t_f}^{t_r} PR(t) dt}. \quad (12)$$

The resilience by recovery is calculated as the ratio of the area between the actual system performance function $P(t)$ and the time axis (the area shaded with downward diagonal stripes in Figure 2) for the time period $t_r \leq t \leq t_h$, and the area between the performance reference function $PR(t)$ and the time axis, for the time period $t_r \leq t \leq t_h$, with $t_h \geq t_r$, i.e., from the start of restoration to the end of the time horizon $H_h - H_r = t_h - t_r$, i.e., within the recovery phase:

$$R_r = \frac{\int_{t_r}^{t_h} P(t) dt}{\int_{t_r}^{t_h} PR(t) dt}. \quad (13)$$

The overall level of system resilience, i.e., the total resilience R_t , is given by the ratio of the area between the actual system performance function $P(t)$ and the time axis for the time period $t_f \leq t \leq t_h$, and the area between the performance reference function $PR(t)$ and the time axis, for the time period $t_f \leq t \leq t_h$, with $t_h \geq t_f$, within the mitigation and recovery phases:

$$R_t = \frac{\int_{t_f}^{t_h} P(t) dt}{\int_{t_f}^{t_h} PR(t) dt}. \quad (14)$$

3 Sensitivity analysis-driven importance measure (SADIM)

3.1 Introduction to SADIM

Generally speaking, we can consider the system model:

$$Z = f(Q), \mathbb{R}^n \rightarrow \mathbb{R}^m, \quad (15)$$

where Z is the set of output variables (OVs) of the model, and Q is the set of uncertain input variables (IVs). In the case of ICIs, IVs include system initial conditions, parameters of the process temporality and parameters related to the failure-recovery process of the system elements, as discussed in Section 2.3, and the OVs include the system resilience metrics, just introduced in Section 2.4.

The uncertainty in IVs propagates to uncertainty on the system resilience metrics (OVs). Sensitivity analysis (SA) can be used to quantitatively evaluate the contributions of the IVs on the OVs, and

identify the most critical/important elements to which higher priority should be given in the protection and recovery strategies design and implementation.

A sensitivity analysis-driven importance measure (SADIM) can be introduced to filter the least relevant input variables and simplify the model in order to reduce computational cost, while maintaining the accuracy needed for the analysis [13]. The filtering criteria can be, for example, a threshold for the unity-based normalized SA indicators defined as $\sigma = 1/n$, where n is the number of IVs [47]. It's also possible to select the most important IVs with respect to a certain percentage of the IVs number [16].

The IVs most relevant to system resilience are related to the elements whose failures most affect the system resilience: then, SADIM can also be used to identify the system critical elements, which are more worthy of investment for system resilience improvement.

3.2 Two strategies to accelerate SADIM computation

The cost for combining SADIM can be very expensive because of the high computation time required by each simulation of the dynamic model (for example, a simulation of a failure scenario for the case study illustrated in Section 4.1 takes around 10 seconds to run and the computational time increases with the growth of the system size; the simulations are carried out by using Yalmip Toolbox [48] and Cplex optimizer [49] on Matlab 2015a, on an Intel® Core™ 2 Duo CPU E7600 @ 3.07 GHz) and the large number of simulations required by SA (for example, more than 10^6 Monte Carlo simulations are required in SA approaches that use a distribution-based SA indicator [18]).

To reduce the computational burden, we propose two strategies, as shown in Figure 3. In the first approach (referred in the following as SADIM 1), we adopt a fast-running Artificial Neural Network (ANN) regression model to replace the original time-consuming dynamic model **and, then, we apply the SA considering a variance-based sensitivity index (i.e., the first-order index) on the ANN model outputs.** In the second approach (referred in the following as SADIM 2), we keep the long-running dynamic model, but we reduce the number of simulations necessary for an accurate SA by implementing an ensemble-based approach [16] in the SADIM. In the ensemble-based approach, three SA indicators are computed and, then, aggregated to produce a reliable ranking of the most critical elements [16].

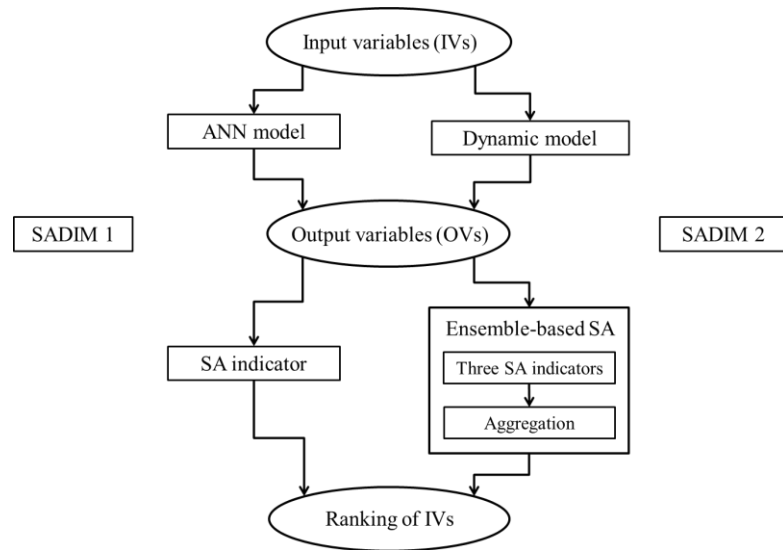


Figure 3 Approaches to reduce the computational burden for the sensitivity analysis-driven importance measure calculation.

3.2.1 Artificial Neural Networks

An ANN is a modelling structure composed of many parallel computing nodes arranged in different layers and interconnected by weighed connections [50]. The node in an ANN performs few and simple operations and communicates the results to its neighboring nodes. From a mathematical viewpoint, ANNs consist of a set of nonlinear (e.g., sigmoidal) basis functions with adaptable parameters that are adjusted by a training process (on many different input/output data examples), i.e., an iterative process of regression error minimization [51]. ANNs have been proved to be a powerful technique to perform massively parallel computations for data processing [52] and to solve a variety of problems in prediction, control, optimization, pattern recognition, etc. [53]. Specifically, ANNs have been demonstrated to be universal approximants of continuous nonlinear functions (under mild mathematical conditions) [54], i.e., in principle, an ANN model with a properly selected architecture can be a consistent estimator of any continuous nonlinear function. Further details about ANN regression models are not reported here for brevity; the interested reader may refer to the cited references and the copious literature in the field.

In this work, we consider the classical three-layered, feed-forward ANN composed of three layers (input, hidden and output, see Figure 1) and trained by the error back-propagation algorithm. Notice that it is a good practice to model the system using as little number of hidden layers as possible to keep the number of parameters to be estimated as low as possible: indeed, the higher the number of hidden

layers, the larger the model complexity and the poorer the generalization capabilities [55]. In addition, too many parameters will drastically slow down the learning process [56].

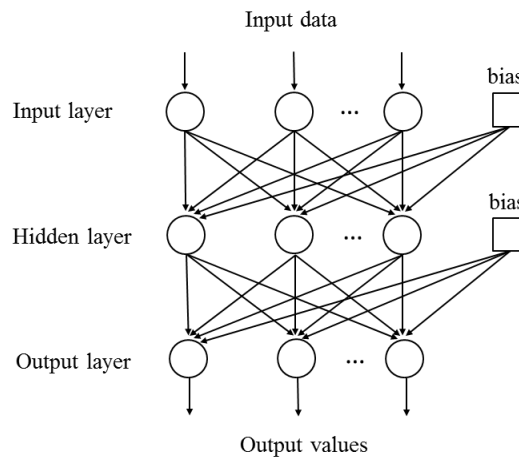


Figure 4 Layout of a three-layered, feed-forward Artificial Neural Network.

The numbers of nodes in the input layer and the output layer are known, as they correspond to the numbers of IVs and OVs. The number of nodes in the hidden layer has to be determined during the training process; in general, also this number, as the number of hidden layers, is kept as low as possible, since the higher the number of hidden nodes the higher the number of parameters to be estimated. In general, an ANN with too few hidden nodes does not succeed in learning the training data set; vice versa, an ANN with too many hidden nodes learns the training data set too well, and it does not have generalization capability [33].

Typically, the entire set of input-output data is divided into three subsets: a training (input/output) data set, used to calibrate the parameters of the ANN regression model (i.e., the weights of the links); a validation (input/output) data set, used to monitor the accuracy of the ANN model during the training procedure; a test (input/output) data set, not used during ANN training and validation, but used at the very end of the training to evaluate the network generalization capability when fed with new data. ANNs are good at interpolation, but they can be very bad at extrapolation; to guarantee that the bounds of the training domain are not exceeded, data must not be over-fitted during the training process. This can be guaranteed by the validation process: in practice, the validation error is computed on the validation set at different iterative stages of the training procedure: at the beginning of training, this value decreases as does the error computed on the training set; later in the training, if the ANN regression model starts over-fitting the data, the error calculated on the validation set starts increasing

and the training process must be stopped [50]. The Root Mean Square Error (RMSE) on the training, validation and test data set has been considered for the ANN development in this paper.

A final remark is in order with respect to application to large-scale systems. In this work, a small case study has been considered, but it is worth mentioning that issues related with the high dimensionality of the input parameter space can arise when considering large-scale systems. Indeed, any algorithm involving the construction of a metamodel suffers when the dimensionality of the input parameter (i.e., feature) space increases, because the available set of input-output data examples becomes sparser with a power law relationship [57]. This issue is unavoidable and limits the application of any algorithm for metamodeling in engineering problems, unless dimensionality reduction strategy is adopted (e.g., principal component analysis, or feature extraction and selection) [33].

3.2.2 *Ensemble-based sensitivity analysis*

The ensemble method allows combining the output of three single SA indices to identify reliable rankings [16]. As a consequence, the resulting ranking overcomes the problem of possible misinterpretations of the individual methods, specifically in cases of limited quantity of data [16]. In Section 3.2.2.1, the three SA indicators used in the ensemble approach are illustrated and in Section 3.2.2.2, the method proposed to aggregate the results is described.

3.2.2.1 *Sensitivity analysis indicators*

In this work, the three SA indicators considered in the ensemble-based SA method are: 1) first-order variance-based sensitivity measure (also called Pearson's correlation ratio or Sobol's first-order index) [19,34]; 2) distribution-based sensitivity measure [18] and 3) Beta measure on the basis of Kolmogorov-Smirnov distance [35]. The first index is variance-based, whereas the last two indices are given by moment independent techniques.

Methods based on variance decomposition are the most used for global SA [16]; indeed, they are suitable for complex nonlinear models since they do not introduce any hypothesis on the model functional relationship to its inputs [15,16,17,18]. Variance-based methods explore the entire range of variation of the inputs that are modelled as stochastic variables inducing variability (uncertainty) in the model outputs. The variance of the output distributions is considered a good proxy of the output uncertainty [15]. However, the assumption that a single moment of the output distribution, i.e., the variance, is sufficient to describe output variability is not always appropriate, e.g., in case of multi-modal or highly-skewed distributions [15,16,17,18,58]. To overcome this limitation, moment independent techniques, such as distribution-based sensitivity measure and Beta measure on the basis of Kolmogorov-Smirnov distance, do not consider only one specific moment of the output distribution, but

they look at the entire output distribution in a moment independent fashion [15,18]. Specifically, the distribution-based sensitivity measure and the Beta measure on the basis of Kolmogorov-Smirnov distance are based on the distance between the unconditional output distribution (generated by varying all inputs) and the conditional (on a given input) output distribution.

In the following, the mathematical formulation of the three SA indicators considered in the ensemble-based SA method is given.

Let Z_j denote one of the OVs and Q_i one of IVs, the first-order variance-based sensitivity index, S_i , is defined as [19,34]:

$$S_i = \frac{V[E(Z_j|Q_i)]}{V[Z_j]}. \quad (16)$$

where $V[Z_j]$ is the variance of the model uncertain OV, and $V[E(Z_j|Q_i)]$ is the variance of the expected value of Z_j if the impact from Q_i is eliminated, i.e., assuming that Q_i is fixed at its “true” value. This first-order index represents the direct contribution of each IV to the variance of OV.

The distribution-based indicator, δ_i , is given by [18]:

$$\delta_i = \frac{1}{2} E[s(Q_i)], \quad (17)$$

where $s(Q_i)$ is defined as:

$$s(Q_i) = \int |f_{Z_j}(z_j) - f_{Z_j|Q_i}(z_j)| dz_j, \quad (18)$$

where $f_{Z_j}(z_j)$ is the density function of Z_j , and $f_{Z_j|Q_i}(z_j)$ is the conditional probability density function of Z_j when Q_i is a fixed value. The distribution-based SA indicator δ_i represents the expected shift in the distribution of Z_j provoked by Q_i . Unlike the first-order variance-based sensitivity index S_i , which considers one moment of the OV distribution, the indicator δ_i accounts for the entire distributions of OVs. Applications show that S_i and δ_i are in agreement in identifying the less relevant IVs, but discrepancies exist in the ranking of the most relevant ones [18].

The Beta measure, β_i , based on the Kolmogorov-Smirnov distance, is computed by averaging the distance between the unconditional and conditional (on a given input) distributions of the output as follows [35]:

$$\beta_i = E[\sup_{z_j \in \Omega_{Z_j}} |F_{Z_j}(z_j) - F_{Z_j|Q_i}(z_j)|]. \quad (19)$$

where $F_{Z_j}(z_j)$ is the cumulative distribution function (CDF) of Z_j and $F_{Z_j|Q_i}(z_j)$ is the conditional CDF of Z_j when Q_i is a fixed value. The metric $\sup_{z_j \in \Omega_{Z_j}} |F_{Z_j}(z_j) - F_{Z_j|Q_i}(z_j)|$ in Eq. (19) is the Kolmogorov-Smirnov distance, which is defined as the largest absolute difference between the two CDFs, and has the property to be scale invariant.

The main advantage of the Beta measure, β_i , compared to the distribution-based indicator, δ_i , is in the use of CDFs rather than density functions. Indeed, CDFs can be defined for all distributions (even if a

distribution does not admit a density) and they allow relating the sensitivity measure to, e.g., the probabilities of exceeding a target [35].

In this work, the three SA indicators have been applied to the same input-output data obtained from system behaviour simulations, so they have been calculated without the need of rerunning the model, avoiding extra computational cost.

3.2.2.2 Aggregated ranking of sensitivity indicators

The three SA indicators introduced in Section 3.2.2.1 are aggregated for the final ranking of the IVs that affect the OVs. We take as reference the ranking sum aggregation [36] and propose the following method to aggregate the values of the three SA indicators S_i , δ_i and β_i in one SA indicator I_i . For each IV, Q_i , the aggregated SA indicator I_i is calculated as follows:

- 1) For each SA indicator, SA_i , i.e., S_i , δ_i or β_i , rescale its original value to a normalized value $SA_i^* = \frac{SA_i}{\sum_i SA_i}$, which is the ratio of the SA indicator value of an IV Q_i over the sum of the SA indicator values of all the IVs. This step brings the values of different SA indicators into the range [0,1].
- 2) Calculate the sum of the results obtained in step 1), $SSA_i = S_i^* + \delta_i^* + \beta_i^*$.
- 3) Normalize the values of SSA_i to the aggregated SA indicator $I_i = \frac{SSA_i}{\sum_i SSA_i}$.

This aggregation method considers the direct integration of the results of the different SA indicators, i.e., it calculates the sum of values of SA indicators instead of the sum of ranking, as in the ranking sum aggregation method. The ranking sum aggregation method may lead to practical undesirable situations: indeed, it can lead to multiple IVs occupying the same ranking position. Comparing to the ranking sum aggregation method, the advantage of the proposed aggregation method is that it is able to capture the variability of IVs with respect to different SA indicators, avoiding the situation of multiple IVs in the same ranking position.

4 Case study and results

4.1 Interconnected natural gas distribution network and electric power grid

The case study is taken from [59] and considers two ICIs: a natural gas distribution network and an electric power grid (Figure 5, solid and dash-dotted lines, respectively). The objective is to provide the necessary amount of gas and electricity to the demand nodes. In particular, the gas distribution network supplies gas to two users, D_1 and D_2 , and to two electric power generators, E_1 and E_2 , that provide electricity to two users of electricity, L_1 , and L_2 .

The natural gas distribution network has two suppliers, S_1 and S_2 , whose outputs are assumed to be equal to 90000 cubic feet, i.e., 90 MCF (1 MCF \approx 28.32 m³), and 180 MCF, respectively; two buffers (gas reservoirs), DS_1 and DS_2 ; five transporters a , b , c , d and e ; and two users D_1 and D_2 , whose demands, D_{D1} and D_{D2} , are equal to 100 MCF and 80 MCF, respectively. The electric power network has two converters (electric power generators), E_1 and E_2 , that transform gas into electricity with a constant coefficient β , where $\beta=10$ MWh/MCF, i.e., 1 MCF of natural gas produces 10 MWh of electricity; two transporters, G_1 and G_2 ; two users L_1 and L_2 , whose demands, D_{L1} and D_{L2} , are equal to 500 MWh and 400 MWh, respectively.

In this case study, we consider the same failure scenario as in [59], where the vulnerable elements, which are highlighted in Figure 5, fail due to a disruption event. The uncertainties of IVs, i.e., system design parameters, parameters related to the process temporality, failure magnitudes and recovery rates of the vulnerable elements identified in [59], are considered as described by uniform distributions, for illustration purposes. The ranges of the distributions are reported in Table 1.

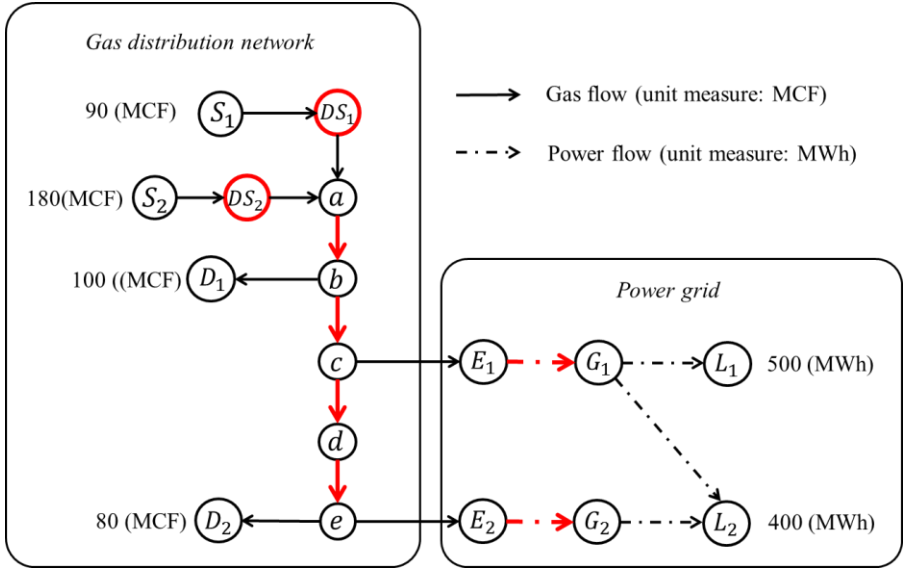


Figure 5 Interconnected natural gas-power systems (vulnerable nodes and links are highlighted).

TABLE 1
Ranges of uncertain input variables (1 MCF \approx 28.32 m³)

Description	Symbol	Interval	Unit measure
Response time	H_r	[0, 30]	hrs
Time horizon	H_h	[50, 120]	hrs
Initial storage of buffer DS_1	$x_{DS_1}^{t=0}$	[1000, 4000]	MCF
Initial storage of buffer DS_2	$x_{DS_2}^{t=0}$	[2000, 8000]	MCF
Failure magnitude of supplier S_1	F_1	[0, 90]	MCF
Failure magnitude of supplier S_2	F_2	[0, 180]	MCF
Failure magnitude of link L_{a-b}	F_3	[0, 300]	MCF
Failure magnitude of link L_{b-c}	F_4	[0, 170]	MCF
Failure magnitude of link L_{c-d}	F_5	[0, 100]	MCF
Failure magnitude of link L_{d-e}	F_6	[0, 100]	MCF
Failure magnitude of link $L_{E_1-G_1}$	F_7	[0, 800]	MWh
Failure magnitude of link $L_{E_2-G_2}$	F_8	[0, 400]	MWh
Recovery rate of supplier S_1	μ_1	[0, 1.8]	MCF/hrs
Recovery rate of supplier S_2	μ_2	[0, 3.6]	MCF/hrs
Recovery rate of link L_{a-b}	μ_3	[0, 6]	MCF/hrs
Recovery rate of link L_{b-c}	μ_4	[0, 3.4]	MCF/hrs
Recovery rate of link L_{c-d}	μ_5	[0, 2]	MCF/hrs
Recovery rate of link L_{d-e}	μ_6	[0, 2]	MCF/hrs
Recovery rate of link $L_{E_1-G_1}$	μ_7	[0, 16]	MWh/hrs
Recovery rate of link $L_{E_2-G_2}$	μ_8	[0, 8]	MWh/hrs

4.2 Results by SADIM 1

4.2.1 Artificial Neural Network models

To build the data sets, 5000 IVs have been sampled and the OV's have been calculated by simulating the original dynamic model. The input/output data have been divided into three data sets as follows: 70% (i.e., 3500 data) in the training data set, 15% (i.e., 750 data) in the validation data set and 15% (i.e., 750 data) in the test data set. Training, validation and test have, then, been carried out by the ANN Toolbox of Matlab 2015a.

Three different ANN models have been built, with each one output node representing one of the three system resilience measures, R_m , R_r and R_t . Table 2 shows the numbers of hidden nodes of the ANN models found by trial and error, and the Root Mean Square Error (RMSE) values obtained on the training, validation and test data sets.

TABLE 2

Number of hidden nodes of the ANN models and Root Mean Square Error (RMSE) of the training, validation and test data sets for resilience by mitigation R_m , resilience by recovery, R_r , and total resilience, R_t .

	R_m	R_r	R_t
Hidden nodes	30	29	28
RMSE Training	0.0184	0.0406	0.0377
RMSE Validation	0.0249	0.0524	0.0464
RMSE Test	0.0286	0.0532	0.0492

For brevity sake, in the following, we discuss only the results related to the total resilience R_t .

Figure 6 shows the linear regression between the network outputs (total resilience computed by the ANN model, R_t^{ANN} , on the vertical axis) and the original dynamic model outputs (total resilience, R_t^{MPC} , computed by the MPC, on the horizontal axis), with respect to the training, validation, test, and the entire data set. Notice that only the first 50 data are shown in Figure 6, for rendering the Figure visible. For a perfect fit, the data should fall along a 1:1 line, where the network outputs are equal to the targets, i.e., the original dynamic simulations outputs. In this case, the correlation coefficient R_c is always higher than 0.98, which indicates that the fit is good for all data sets. Then, once the ANN is trained, it can provide accurate values of total resilience in correspondence of new input data.

The computational time required by one simulation of the trained ANN model to calculate the total resilience indicator of one failure scenario is around 2×10^{-4} seconds. On the contrary, one simulation of the MPC dynamic model takes 10 seconds.

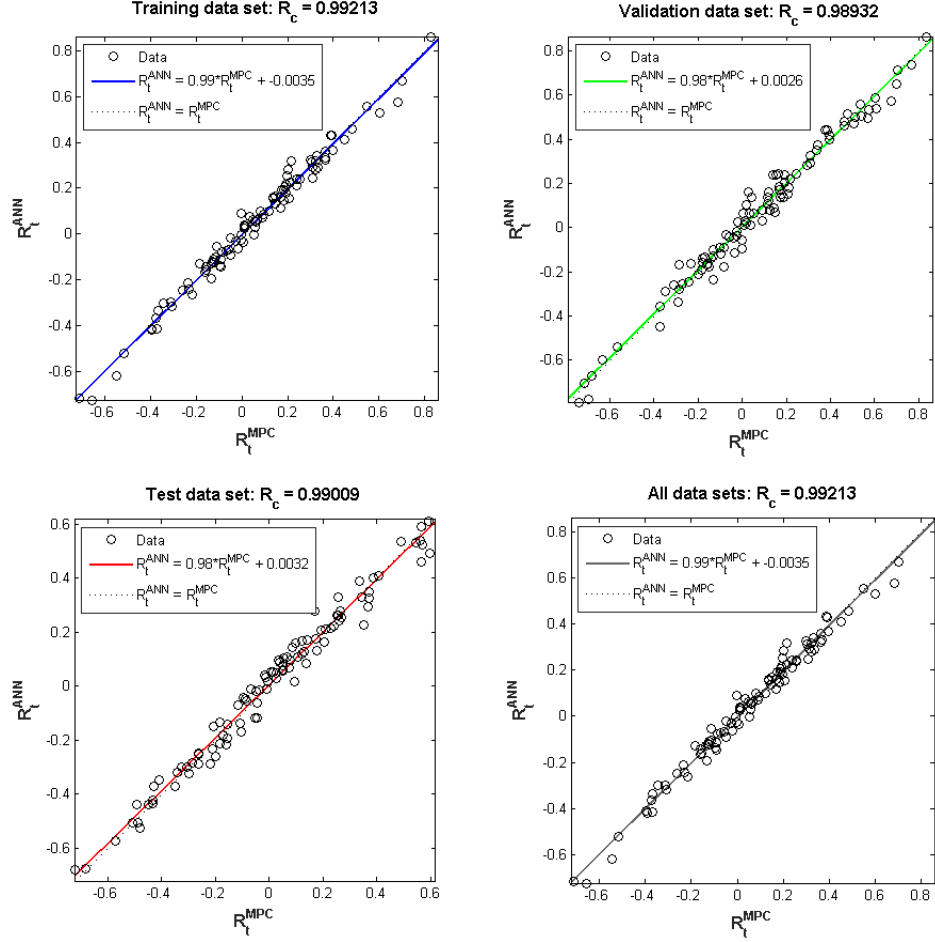


Figure 6. Linear regression between the network outputs (total resilience computed by the ANN model, R_t^{ANN} , on the vertical axis) and the original dynamic model outputs (total resilience, R_t^{MPC} , computed by the Model Predictive Control (MPC), on the horizontal axis).

4.2.2 Input variable importance by sensitivity analysis

For each resilience measure, R_m , R_r or R_t , 5000 simulations by the ANNs have been carried out to estimate unconditional distributions and 10^6 simulations have been run to estimate conditional distributions for each IV. Then, the first-order variance-based SA indicators of each IV have been calculated according to equation (16). In Table 3, the values of the first-order variance-based sensitivity measure computed for the resilience by mitigation, $S_i^{R_m}$, resilience by recovery, $S_i^{R_r}$, and total resilience, $S_i^{R_t}$, are reported. The most important IVs are those whose SA indicator values are larger than threshold $\sigma = 0.05$.

The results of the SA first-order indices for the resilience by mitigation, S_i^{Rm} , resilience by recovery, S_i^{Rr} , and total resilience, S_i^{Rt} , are reported in Table 3.

TABLE 3
SA indicators (first order-indices) of IV for resilience by mitigation, S_i^{Rm} , resilience by recovery, S_i^{Rr} , and total resilience, S_i^{Rt} , computed by means of SADIM 1 approach. The values higher than the threshold value σ are in bold.

IV	SADIM 1		
	S_i^{Rm}	S_i^{Rr}	S_i^{Rt}
H_r	0.1667	0.0496	0.0565
H_h	0.0344	0.0661	0.0519
$x_{Ds_1}^{t=0}$	0.0344	0.0297	0.0336
$x_{Ds_2}^{t=0}$	0.0344	0.0319	0.0351
F_1	0.0344	0.0385	0.0397
F_2	0.0344	0.0705	0.0611
F_3	0.1377	0.1355	0.1481
F_4	0.0523	0.0661	0.0641
F_5	0.0372	0.0319	0.0351
F_6	0.0441	0.0319	0.0366
F_7	0.0785	0.0826	0.0855
F_8	0.0358	0.0286	0.0336
μ_1	0.0344	0.0330	0.0366
μ_2	0.0344	0.0474	0.0427
μ_3	0.0344	0.0595	0.0534
μ_4	0.0344	0.0463	0.0641
μ_5	0.0344	0.0319	0.0351
μ_6	0.0344	0.0319	0.0351
μ_7	0.0344	0.0374	0.0382
μ_8	0.0344	0.0496	0.0336

It can be seen that during the mitigation phase, the most important IVs identified by the SA for the resilience by mitigation, S_i^{Rm} , computed by employing the SADIM 1, are the response time, H_r , and the failure magnitudes, F_3 , F_7 , and F_4 , whose values are higher than the threshold value, σ , (as shown in Table 3, in bold). The results show which are the components and, consequently, the activities that need to be considered to enhance the resilience in the mitigation phase; specifically, in this case, they are related to the improvement of, e.g., failure detection capabilities that can increase the system response, and the strengthening of the robustness of links L_{a-b} , $L_{E_1-G_1}$ and L_{b-c} , to reduce the failure magnitudes.

During the recovery phase, the most relevant IVs identified by the SA for the resilience by recovery, S_i^{Rr} , are the failure magnitudes F_3 , F_7 , F_2 and F_4 , the time horizon H_h , and the recovery rate μ_3 , whose values are higher than the threshold value, σ , (as shown in Table 3, in bold). Then, in this phase, the

most important resilience enhancement activities should focus on the improvement of the emergency preparedness of the users and of the recovery efficiency of link L_{a-b} , $L_{E_1-G_1}$ and L_{b-c} and suppliers S_2 .

Regarding the total resilience, the most relevant IVs identified by the SA, S_i^{Rr} , are the failure magnitudes F_3 , F_7 , F_4 and F_2 , the response time H_r , the time horizon H_h and the recovery rate μ_3 , whose values are higher than the threshold value, σ , (as shown in Table 3, in bold). It can be seen that the most important IVs are the combination of those variables identified for resilience by mitigation and resilience by recovery. This result is coherent with the meaning of total resilience, which represents the resilience level of the system considering both the failure and recovery stages. The corresponding resilience enhancement activities in two phases can be implemented following the results for resilience by mitigation and those for resilience by recovery, respectively.

4.3 Results by SADIM 2

In SADIM 2, the original MPC dynamic model simulations are performed to calculate the values of the resilience measures, i.e., R_m , R_r and R_t . However, the number of Monte Carlo simulations for computing the unconditional and conditional distributions of each IV reduces to 100 and 10^4 , respectively, thanks to the use of the ensemble-based approach. In SADIM 2, the first-order variance-based sensitivity index, the distribution-based indicator, and the Beta measure based on Kolmogorov-Smirnov distance, have been calculated, for each IV, according to equations (16), (17), and (19), respectively, and then have been aggregated, as explained in Section 3.2.2.2.

In Table 4, the values of the ensemble-based sensitivity measure computed for the resilience by mitigation, I_i^{Rm} , resilience by recovery, I_i^{Rr} , and total resilience, I_i^{Rt} , are reported. The relevant IVs are those whose SA indicator values are larger than the threshold $\sigma = 0.05$.

TABLE 4

Ensemble-based SA indicators of the IVs for resilience by mitigation, I_i^{Rm} , resilience by recovery, I_i^{Rr} , and total resilience, I_i^{Rt} , computed by means of SADIM 2 approach. The values higher than the threshold value σ are in bold.

IV	SADIM 2		
	I_i^{Rm}	I_i^{Rr}	I_i^{Rt}
H_r	0.2662	0.0508	0.0580
H_h	0.0303	0.0641	0.0496
$x_{Ds_1}^{t=0}$	0.0293	0.0320	0.0300
$x_{Ds_2}^{t=0}$	0.0310	0.0337	0.0326
F_1	0.0295	0.0350	0.0374
F_2	0.0295	0.0630	0.0577
F_3	0.1452	0.1754	0.2215
F_4	0.0400	0.0530	0.0549
F_5	0.0320	0.0324	0.0308
F_6	0.0384	0.0329	0.0313
F_7	0.0603	0.0764	0.0686
F_8	0.0298	0.0309	0.0298
μ_1	0.0292	0.0346	0.0343
μ_2	0.0292	0.0417	0.0402
μ_3	0.0299	0.0714	0.0595
μ_4	0.0293	0.0411	0.0382
μ_5	0.0303	0.0320	0.0303
μ_6	0.0308	0.0320	0.0299
μ_7	0.0303	0.0357	0.0356
μ_8	0.0294	0.0320	0.0297

During the mitigation phase, the most important IVs identified by the SA for the resilience by mitigation, I_i^{Rm} , identified by employing the SADIM 2, are the response time H_r , and the failure magnitudes F_3 and F_7 , whose values are higher than the threshold value, σ , (as shown in Table 4, in bold). Therefore, the most important resilience enhancement activities include, e.g., the improvement of failure detection capability to reduce the response time and the strengthening of the robustness of links L_{a-b} and $L_{E_1-G_1}$.

During the recovery phase, the most important IVs identified by the SA for the resilience by recovery, I_i^{Rr} , identified by employing the SADIM 2, are the failure magnitudes F_3 , F_7 , F_2 and F_4 , the recovery rate μ_3 , the time horizon H_h , and the response time H_r , whose values are higher than the threshold value, σ , (as shown in Table 4, in bold). Then, the important resilience enhancement activities should focus on the improvement of the failure detection capability, the emergency preparedness of the users and the recovery efficiency of links L_{a-b} , $L_{E_1-G_1}$, and L_{b-c} , and suppliers S_2 .

Regarding the total resilience, the most relevant IVs identified by the SA, I_i^{Rt} , are the failure magnitudes F_3, F_7, F_2 and F_4 , the recovery rate μ_3 , and the response time H_r , whose values are higher than the threshold value, σ , (as shown in Table 4, in bold).

The most important IVs are the combination of those variables identified for resilience by mitigation and resilience by recovery, except for the time horizon H_h , whose value is equal to 0.0469. The corresponding resilience enhancement activities can be implemented in the mitigation and recovery phases according to the individual results for resilience by mitigation and resilience by recovery, respectively.

4.4 Comparison of SADIM approaches

The results given by SADIM 1 (Section 4.2.2) and SADIM 2 (Section 4.3) are compared with those obtained by a given data estimation SA method [19], (SADIM 3), in Section 4.4.1. Then, considerations about the computational cost and the effectiveness of the three methods are given in Sections 4.4.2 and 4.4.3, respectively. SADIM 3 has been applied by considering 5000 system responses generated by the original dynamic model and Monte Carlo simulation. Further details on the results given by SADIM 3 can be found in [60].

4.4.1 Ranking of important IVs

The most important IVs and subsystems can be ranked on the basis of the SA indicator values. In Table 5, the five most important IVs, i.e., those with larger SA indicator values, identified by the three SADIM approaches, are given with respect to the three resilience measures (resilience by mitigation, R_m , resilience by recovery, R_r , and total resilience, R_t).

TABLE 5
Rankings of the five most important IVs given by SADIM 1, SADIM 2 and SADIM 3 approaches for resilience by mitigation R_m , resilience by recovery, R_r , and total resilience, R_t

	R_m			R_r			R_t		
	SADIM 1	SADIM 2	SADIM 3	SADIM 1	SADIM 2	SADIM 3	SADIM 1	SADIM 2	SADIM 3
1	H_r	H_r	H_r	F_3	F_3	F_3	F_3	F_3	F_3
2	F_3	F_3	F_3	F_7	F_7	F_7	F_7	F_7	F_7
3	F_7	F_7	F_7	F_2	μ_3	H_h	F_4	μ_3	F_2
4	F_4	F_4	F_4	H_h	H_h	F_2	F_2	H_r	F_4
5	F_6	F_6	F_6	F_4	F_2	F_4	H_r	F_2	H_h

For the resilience by mitigation R_m , the five most important IVs obtained by SADIM 1 and 2 methods are identical with those obtained by SADIM 3: they are the response time, H_r , and the failure magnitudes F_3, F_7, F_4 and F_6 , which reflect the importance of protection efforts on links $L_{a-b}, L_{E_1-G_1}, L_{b-c}$ and L_{d-e} .

For the resilience by recovery R_r , the most important two IVs, obtained by the three SADIM methods, are F_3 and F_7 , related to the failure magnitudes of link L_{a-b} and link $L_{E_1-G_1}$. The other three most important IVs are the same for SADIM 1 and SADIM 3 (even if they are in a different order) and they are: time horizon, H_h , failure magnitude of supplier S_2, F_2 , and failure magnitude of link L_{b-c}, F_4 . The approach SADIM 2, instead, identifies also the recovery rate of link L_{a-b}, μ_3 , as important.

If we look through the entire failure-recovery process (i.e., with respect to the total resilience), it can be seen that three IVs, i.e., F_3, F_7 , and F_2 , have been identified as critical by all the three SADIM methods, and, specifically, F_3 and F_7 , are the most critical. The other IVs that appear in the top five by at least one SADIM method are: F_4, μ_3, H_r, H_h . The importance of F_4 is supported by SADIM 1 and 3; the criticality of the response time, H_r is highlighted by SADIM 1 and 2; whereas the importance of the recovery rate, μ_3 , and the time horizon, H_h , is supported by only one method, i.e., SADIM 2 and SADIM 3, respectively.

The results of SADIM approaches provide different ranking positions of the IVs, which indicate the priorities of the corresponding resilience enhancement activities. In general, topology modification, redundancy allocation of the important elements, failure detection capability are some of the activities that can be implemented to increase the resilience by mitigation. In this specific case, the most important resilience enhancement activities can include the improvement of failure detection capability to reduce the response time and the strengthening of the robustness of links on links $L_{a-b}, L_{E_1-G_1}, L_{b-c}$ and L_{d-e} . Instead, the increase of the recovery efficiency is a typical activity to improve the resilience by recovery by improving the repair rate efficiency of failed elements and/or identifying the best repair sequence (by optimization).

Notice that for the system under analysis, the most important components for resilience are mainly associated with failure magnitudes, response time and time horizon. Indeed, the initial storage of the two buffers and the recovery rates (except for one recovery rate over eight) are not in the ranking of the five most important variables. It is worth mentioning that these results are for the specific system analyzed and cannot be generalized to any interconnected critical infrastructure system.

4.4.2 Computational costs of three SADIM approaches

The three applied SADIM methods can significantly reduce the computational cost, comparing to the conventional method with the original dynamic model and large numbers of simulations in SA. Indeed,

to obtain the above results, the traditional SA method requires 2×10^7 simulations, i.e., it takes around 5000 hours, whereas, the SADIM 1 and SADIM 3 methods require 5000 simulations of the original MPC dynamic model, which takes around 13 hours, and the SADIM 2 method needs 10^4 simulations to obtain the SA indicator for each IV, i.e., it takes around 26 hours, the double of time required by SADIM 1 and 3. Notice that the computational cost of SADIM 1 does not depend on the number of system parameters, i.e., it does not increase if the number of IVs increases; on the contrary, the computational cost of SADIM 2 strongly depends on the number of IVs. Then, SADIM 1 and 3 are better than SADIM 2 with the respect to the computational cost.

4.4.3 Effectiveness of three SADIM approaches

The SADIM methods provide the rankings of the most important/critical parameters with respect to system resilience, which can, then, be improved efficiently by taking into account the results given by these methods. In the following, we take into account the results obtained in Section 4.3 in order to improve the system resilience of the ICIs given in Section 4.1; then, the effectiveness of the three SADIM methods are compared.

We consider first an initial configuration (the reference case) of the IVs in which all of them are assumed to take their mean values (see Table 1). Then, we modify these values according to the ranking position of the IVs given by each SADIM method in order to analyze the improvement on the resilience by mitigation, R_m , resilience by recovery, R_r , and total resilience, R_t . The original level of an IV increases, e.g., in the case of the recovery rate, or reduces, e.g., in the case of the failure magnitude or response time, by 50% if it ranks first, by 40% if it ranks second, by 30% if it ranks third, by 20% if it ranks fourth and by 10% if it ranks fifth.

The values of the resilience measures of the reference case and improved values as guided by three SADIM methods are reported in Table 6. As expected, the resilience measure values, R_m , R_r and R_t , increase by applying the resilience strategies identified by the SADIM methods and, in particular, the highest improvement (values in bold in Table 6) are given by SADIM 2 with respect to the resilience by mitigation and by SADIM 1 with respect to the resilience by recovery and total resilience.

Notice that the percentage values adopted to increase the performance of the most important elements have been arbitrarily chosen only for illustration purposes. In real cases, the best strategy for mitigation and/or recovery should be identified for the different types of components.

TABLE 6

Values of resilience measures (resilience by mitigation, R_m , resilience by recovery, R_r , and total resilience, R_t) under the initial condition (reference case) and the SADIM-improved conditions.

	R_m	R_r	R_t
Initial conditions (reference case)	0.6735	0.7482	0.7343
SADIM 1-improved conditions	0.7258	0.8418	0.8243
SADIM 2-improved conditions	0.7733	0.7993	0.7962
SADIM 3-improved conditions	0.6943	0.8363	0.8119

In Figure 7, the evolution in time of the ICIs performance functions, under initial conditions and SADIM-improved conditions, is shown. These curves reflect the characteristics of the failure and recovery processes of the system performance. Due to different recovery start and end instants of the users, the recovery curves of the system performance are not smooth. The slope changes depend on the topological structure of the system, the coefficient values in the dynamic equations and, most importantly, the setting of the system parameters.

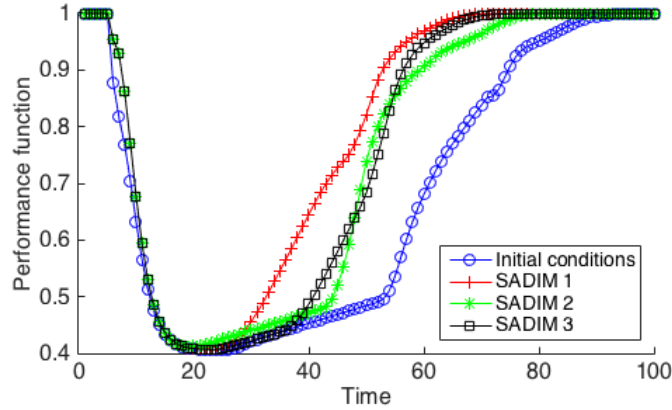


Figure 7. Comparison of the evolution in time of the performance functions of the case study illustrated in Section 4.1 under the initial condition (reference case) and SADIM-improved conditions.

It can be noticed that all the SADIM methods provide useful indications on the improvement of the system resilience of the considered ICI. In particular, the most significant improvement in the performance function is achieved by implementing the resilience strategy guided by the SADIM 1. Since SADIM 1 has, also, a relatively low computational cost, it turns out to be the best SADIM method for this application.

5 Conclusion

In this work, we have developed sensitivity analysis-driven importance measure (SADIM) approaches to identify the most influential system parameters and most critical subsystems with respect to system resilience, within a control-based modelling framework. Three resilience measures have been considered to assess the system resilience of ICIs, i.e., 1) resilience by mitigation R_m , which represents the capacity of resistance of ICIs during the failure phase of the system, 2) resilience by recovery R_r , which measures the capacity of restoration of ICIs during the recovery phase, 3) total resilience R_t , which evaluates the overall resilience performance of ICIs during the failure and recovery phases.

Due to the long simulation time needed to evaluate the dynamic model and the large number of iterations required by the SA, the computational cost of SADIM for large-scaled ICIs is very expensive. To address this issue, we have proposed two approaches and applied them to a case study of interest. The first one, i.e., SADIM 1, consists in employing fast-running ANN models to replace the long-running dynamic model. The second approach, i.e., SADIM 2, aims at reducing the number of simulations required for SA. It adopts an ensemble-based method that aggregates three different SA indicators, which can be calculated by employing a smaller number of simulations. This approach uses the original, costly, dynamic model but reduces the number of simulations for SA.

We have applied the proposed SADIM approaches (SADIM 1 and 2) and a given data estimation SA approach (SADIM 3) to a case study concerning a gas supply system and a power grid. The computational cost and the effectiveness of the SADIM methods have been compared:

- With respect to the computational cost, both the proposed SADIM methods can largely reduce the computational burden of the conventional SA method. SADIM 1 is faster than SADIM 2, but slower than SADIM 3, due to the training of the ANN models.
- With respect to effectiveness, the results obtained from SADIM 1 lead to a larger improvement of system resilience than those provided by SADIM 2 and SADIM 3.

For the case study considered, SADIM 1, which integrates the used of ANN estimation in the standard process of SA, has turned out to be the best SADIM method. To generalize this finding to other systems, more ICIs should be analyzed and, in addition, the uncertainty introduced by the use of ANNs should be addressed.

With the capability of the proposed SADIM approaches, one direction of future work is the optimization of the resilience improvement strategies for ICIs on the basis the results of SADIM.

Acknowledgement

This study has been partially sponsored by the Chilean National Commission for Scientific and Technological Research (CONICYT) under FONDECYT Grant #3180464 (FONDECYT Postdoctorado) and by the Chilean National Research Center for Integrated Natural Disaster Management (CIGIDEN) CONICYT/FONDAP/15110017.

References

1. Ouyang, Min, Leonardo Dueñas-Osorio, and Xing Min. 2012. "A Three-Stage Resilience Analysis Framework for Urban Infrastructure Systems." *Structural Safety* 36–37. Elsevier Ltd: 23–31.
2. Cimellaro, Gian Paolo, Andrei M. Reinhorn, and Michel Bruneau. 2010. "Framework for Analytical Quantification of Disaster Resilience." *Engineering Structures* 32 (11). Elsevier Ltd: 3639–49. doi:10.1016/j.engstruct.2010.08.008.
3. Lee, Earl E., John E. Mitchell, and William A. Wallace. 2007. "Restoration of Services in Interdependent Infrastructure Systems: A Network Flows Approach." *IEEE Transactions on Systems, Man and Cybernetics Part C: Applications and Reviews* 37 (6): 1303–17.
4. Ouyang, Min. 2014. "Review on Modeling and Simulation of Interdependent Critical Infrastructure Systems." *Reliability Engineering and System Safety* 121: 43–60.
5. Zio, Enrico. 2016. "Challenges in the Vulnerability and Risk Analysis of Critical Infrastructures." *Reliability Engineering and System Safety* 152 (August). Elsevier: 137–50.
6. SRA. 2015. "Society of Risk Analysis, Glossary of the Specialty Group on Foundations of Risk Analysis," <http://www.sra.org/news/sra-develops-glossary-risk>.
7. Hosseini, Seyedmohsen, Kash Barker, and Jose E. Ramirez-Marquez. 2016. "A Review of Definitions and Measures of System Resilience." *Reliability Engineering and System Safety* 145: 47–61. doi:10.1016/j.res.2015.08.006.
8. Rose, A., 2007. Economic resilience to natural and man-made disasters: Multidisciplinary origins and contextual dimensions. *Environmental Hazards*, 7(4), pp.383–398.
9. Zobel, C.W., 2011. Representing perceived tradeoffs in defining disaster resilience. *Decision Support Systems*, 50(2), pp.394–403.
10. Fang, Y.P., Pedroni, N. & Zio, E., 2016. Resilience-Based Component Importance Measures for Critical Infrastructure Network Systems. *IEEE Transactions on Reliability*, 65(2), pp.502–512.
11. Liu, Xing, Elisa Ferrario, and Enrico Zio. 2017. "Resilience Analysis Framework for Interconnected Critical Infrastructures." *ASCE-ASME J. Risk and Uncert. in Engrg. Sys., Part B: Mech. Engrg.* 3 (2): 21001. doi:10.1115/1.4035728.

12. Liu, Xing, Yiping Fang, Ionela Prodan, and Enrico Zio. 2017. "A Dynamic Control-Based Modelling Framework for the Resilience Analysis of Interdependent Critical Infrastructures (under Review)." *IEEE Systems Journal*.
13. Saltelli, Andrea. 2005. "Global Sensitivity Analysis: An Introduction." *Sensitivity Analysis of Model Output*, 27–43.
14. Saltelli, A, M Ratto, T Andres, F Campolongo, J Cariboni, D Gatelli, M Saisana, and S Tarantola. 2008. *Global Sensitivity Analysis: The Primer*. John Wiley & Sons.
15. Francesca Pianosi, Keith Beven, Jim Freer, Jim W. Hall, Jonathan Rougier, David B. Stephenson, Thorsten Wagener. 2016. Sensitivity analysis of environmental models: A systematic review with practical workflow. *Environmental Modelling & Software*, 79, pp. 214-232
16. Francesco Di Maio, Giancarlo Nicola, Enrico Zio, and Yu Yu. 2014. "Ensemble-Based Sensitivity Analysis of a Best Estimate Thermal Hydraulics Model: Application to a Passive Containment Cooling System of an AP1000 Nuclear Power Plant." *Annals of Nuclear Energy* 73: 200–210. doi:10.1016/j.anucene.2014.06.043.
17. Tian, W.. 2013. A review of sensitivity analysis methods in building energy analysis. *Renewable and Sustainable Energy Reviews*, 20, pp. 411-419
18. Borgonovo, E. 2007. "A New Uncertainty Importance Measure." *Reliability Engineering & System Safety* 92 (6): 771–84. doi:10.1016/j.ress.2006.04.015.
19. Plischke, Elmar, Emanuele Borgonovo, and Curtis L. Smith. 2013. "Global Sensitivity Measures from given Data." *European Journal of Operational Research* 226 (3): 536–50. doi:10.1016/j.ejor.2012.11.047.
20. Cardoso, J. B., de Almeida, J. R., Dias, J. M., and Coelho, P. G. 2008. Structural reliability analysis using Monte Carlo simulation and neural networks. *Advances in Engineering Software*, 39(6), 505-513.
21. Pedroni, N., Zio, E., and Apostolakis, G. E. 2010. Comparison of bootstrapped artificial neural networks and quadratic response surfaces for the estimation of the functional failure probability of a thermal-hydraulic passive system. *Reliability Engineering & System Safety*, 95(4), 386-395.
22. Bichon, B. J., Eldred, M. S., Swiler, L. P., Mahadevan, S., and McFarland, J. M. 2008. Efficient Global Reliability Analysis for Nonlinear Implicit Performance Functions. *AIAA Journal*, 46(10), 2459-2468.
23. Villemonteix, J., Vazquez, E., and Walter, E. 2009. An informational approach to the global optimization of expensive-to-evaluate functions. *Journal of Global Optimization*, 44(4), 509-534.
24. Bucher, C., and Most, T. 2008. A comparison of approximate response functions in structural reliability analysis. *Probabilistic Engineering Mechanics*, 23(2-3), 154-163.

25. Liel, A. B., Haselton, C. B., Deierlein, G. G., and Baker, J. W. 2009. Incorporating modeling uncertainties in the assessment of seismic collapse risk of buildings. *Structural Safety*, 31(2), 197-211.
26. [Ciriello et al., 2013] Ciriello V, Di Federico V, Riva M, Cadini F, De Sanctis J, Zio E, et al. Polynomial chaos expansion for global sensitivity analysis applied to a model of radionuclide migration in a randomly heterogeneous aquifer. *Stoch Env Res Risk Assess* 2013;27(4):945–54.
27. [Sudret and Mai, 2015] Sudret B, Mai CV. Computing derivative-based global sensitivity measures using polynomial chaos expansions. *Reliab Eng Syst Safety* 2015;134:241–50.
28. [Babuska et al., 2010] Babuska I, Nobile F, Tempone R. A stochastic collocation method for elliptic partial differential equations with random input data. *Siam Rev* 2010;52 (2):317–55.
29. [Hurtado, 2007] Hurtado JE. Filtered importance sampling with support vector margin: a powerful method for structural reliability analysis. *Struct Saf* 2007;29 (1):2–15.
30. [Bect et al., 2012] Bect J, Ginsbourger D, Li L, Picheny V, Vazquez E. Sequential design of computer experiments for the estimation of a probability of failure. *Stat Comput* 2012;22(3):773–93.
31. [Dubourg and Sudret, 2014] Dubourg V, Sudret B. Meta-model-based importance sampling for reliability sensitivity analysis. *Struct Saf* 2014;49:27–36.
32. [Zhang, 2015] Zhang LG, Lu ZZ, Wang P. Efficient structural reliability analysis method based on advanced Kriging model. *Appl Math Model* 2015;39(2):781–93.
33. Ferrario, E., Pedroni, N., Zio, E., Lopez-Caballero, F. 2017. Bootstrapped Artificial Neural Networks for the seismic analysis of structural systems. *Structural Safety*, 67, pages 70-84
34. Sobol, I.M. 1993. “Sensitivity Estimates for Nonlinear Mathematical Models.” *Mathematical Modeling and Computational Experiment* 1: 407–14. doi:1061-7590/93/04407-008.
35. Baucells, Manel, and Emanuele Borgonovo. 2013. “Invariant Probabilistic Sensitivity Analysis.” *Management Science* 59 (11): 2536–49. doi:10.1287/mnsc.2013.1719.
36. Kukkonen, Saku, and Jouni Lampinen. 2007. “Ranking-Dominance and Many-Objective Optimization.” 2007 IEEE Congress on Evolutionary Computation, CEC 2007, 3983–90. doi:10.1109/CEC.2007.4424990.
37. Mayne, D. Q., Rawlings, J. B., Rao, C. V., and Sckaert, P. O., 2000, “Constrained Model Predictive Control: Stability and Optimality,” *Automatica*, 36(6), pp. 789–814.
38. Kouvaritakis, B., and Cannon, M., 2015, “Developments in Robust and Stochastic Predictive Control in the Presence of Uncertainty,” *ASCE-ASME J. Risk Uncertainty Eng. Syst., Part B*, 1(2), p. 021003.

39. Rinaldi, Steven M., James P. Peerenboom, and Terrence K. Kelly. 2001. "Identifying, Understanding, and Analyzing Critical Infrastructure Interdependencies." *IEEE Control Systems Magazine* 21 (6): 11–25. doi:10.1109/37.969131.
40. Liu, Yang-Yu, Jean-Jacques Slotine, and Albert-László Barabási. 2011. "Controllability of Complex Networks." *Nature* 473 (7346): 167–73.
41. Holden, R. et al. (2013) 'A network flow model for interdependent infrastructures at the local scale', *Safety Science*, 53, pp. 51–60.
42. Camacho, Eduardo F., and Carlos Bordons Alba. 2013. *Model Predictive Control*. IEEE Transactions on Automatic Control. Springer Science & Business Media.
43. Bruneau, Michel, Stephanie E. Chang, Ronald T. Eguchi, George C. Lee, Thomas D. O'Rourke, Andrei M. Reinhorn, Masanobu Shinozuka, Kathleen Tierney, William A. Wallace, and Detlof Von Winterfeldt. 2003. "A Framework to Quantitatively Assess and Enhance the Seismic Resilience of Communities." *Earthquake Spectra* 19 (4): 733–52. doi:10.1193/1.1623497.
44. Fang, Y.-P., Pedroni, N. & Zio, E., 2014. Comparing Network-Centric and Power Flow Models for the Optimal Allocation of Link Capacities in a Cascade-Resilient Power Transmission Network. *IEEE Systems Journal*, pp.1–12.
45. Eric D. Vugrin, Drake E. Warren, Mark A. Ehlen, and R. Chris Camphouse. (2010) A Framework for Assessing the Resilience of Infrastructure and Economic Systems. K. Gopalakrishnan & S. Peeta (Eds.): *Sustainable & Resilient Critical Infrastructure Sys.*, pp. 77–116.
46. Ayyub, B.M. 2014. Systems resilience for multihazard environments: definition, metrics and valuation for decision making. *Risk Analysis*, 34(2), pp.340-355.
47. Campolongo, Francesca, Andrea Saltelli, and Jessica Cariboni. 2011. "From Screening to Quantitative Sensitivity Analysis. A Unified Approach." *Computer Physics Communications* 182 (4): 978–88. doi:10.1016/j.cpc.2010.12.039.
48. Lofberg, J. 2004. "YALMIP: A Toolbox for Modeling and Optimization in MATLAB." In 2004 IEEE International Conference on Robotics and Automation (IEEE Cat. No.04CH37508), 284–89. IEEE.
49. Cplex. 2015. "Cplex Optimization Studio IBM ILOG [Online]. 2015, Available: <http://www-03.ibm.com/software/products/en/ibmilogcpleoptistud>."
50. Bishop, C. M. 1995. *Neural Networks for pattern recognition*. Oxford University Press.
51. Rumelhart, D. E., Hinton, G. E., and Williams, R. J. 1986. Learning internal representations by error back-propagation. *Parallel distributed processing: exploration in the microstructure of cognition* (vol. 1), Rumelhart, D. E. and McClelland, J. L., eds., Cambridge (MA): MIT Press.

52. Basheer, I. A., and M. Hajmeer. 2000. "Artificial Neural Networks: Fundamentals, Computing, Design, and Application." *Journal of Microbiological Methods* 43 (1): 3–31. doi:10.1016/S0167-7012(00)00201-3.
53. Hornik, Kurt, Maxwell Stinchcombe, and Halbert White. 1989. "Multilayer Feedforward Networks Are Universal Approximators." *Neural Networks* 2 (5): 359–66. doi:10.1016/0893-6080(89)90020-8.
54. Cybenko, G. 1989. Approximation by superpositions of a sigmoidal function. *Mathematics of Control Signals Systems*, 2, 303-314.
55. Shukla, A. ; Tiwari, R. ; Kala, R. 2010. Artificial neural networks. *Studies in Computational Intelligence*, 2010, Vol.307, pp.31-58
56. Rafiq, M.Y., Bugmann, G., Easterbrook, D.J. 2001. Neural network design for engineering applications. *Computer Structures*, 79, pp.1541-1552.
57. Hemez, F. M., and Atamturktur, S. 2011. The dangers of sparse sampling for the quantification of margin and uncertainty. *Reliability Engineering & System Safety*, 96(9), 1220-1231.
58. Saltelli, A., 2002. Sensitivity Analysis for Importance Assessment. *Risk Analysis*, 22(3), pp.579–590.
59. Nozick, L. K., M. A. Turnquist, D. A. Jones, R. D. Davis, and C. R. Lawton. 2005. "Assessing the Performance of Interdependent Infrastructures and Optimising Investments." *Int. J. Critical Infrastructures* 1 (2/3): 144–54.
60. Liu, Xing, Enrico Zio, Emanuele Borgonovo, and Elmar Plischke. 2017. "Global Sensitivity Analysis of a Model for the Resilience Analysis of Interconnected Critical Infrastructures (under Review)." *Risk Analysis*.